Contribution from the Department of Chemistry,
University of Miami, Coral Gables, Florida 33124

Rate of Reaction of $(P(C_6H_{11})_3)_2W(CO)_3$ with py, $P(OMe)_3$, PPh_2Me, and 2,6-Me_2py. Stopped-Flow Kinetic Study of Concerted Reactions at a Sterically Crowded Metal Center

Alberto A. Gonzalez, Kai Zhang, and Carl D. Hoff*

Received November 18, 1988

The rate of reaction of the complexes $(P(C_6H_{11})_3)_2W(CO)_3$ and $(P(C_6D_{11})_3)_2W(CO)_3$ with $P(OMe)_3$ have been measured by stopped-flow kinetics. At 25 °C the hydrogen-substituted complex follows second-order kinetics with $k = 5.45 \times 10^4$ M^{-1} s^{-1} and $\Delta H^{\ddagger} = 4.2$ kcal/mol. An inverse kinetic isotope effect is observed with $k(H)/k(D) = 0.87$. The ligand PPh_2Me reacts 3 times more slowly than $P(OMe)_3$ and shows a larger inverse kinetic isotope effect, $k(H)/k(D) = 0.78$. Reaction of $(P(C_6H_{11})_3)_2W(CO)_3$ with 2,5-dimethylpyridine occurs with the rate constant 8.6×10^3 M^{-1} s^{-1} at 25 °C, 2 orders of magnitude slower than the reaction with pyridine. The unusually high selectivity is ascribed to steric factors at the crowded metal center. New stopped-flow data at low pyridine concentrations are reported for dissociation of pyridine from the complexes $(P(C_6H_{11})_3)_2W(CO)_3(py)$ and $(P(C_6D_{11})_3)_2W(CO)_3(py)$. A primary kinetic isotope effect $k_1(H)/k_1(D) = 1.19$ is observed in these reactions. These results imply that, in spite of the steric crowding at the metal center, dissociation of pyridine is assisted by partial formation of the W···H "agostic" bond in the transition state.

Introduction

Metal centers in active catalysts or enzymes may involve significant steric crowding at the metal. In spite of this there are relatively few reports of "coordinatively unsaturated" organometallic complexes that discriminate with regard to ligand binding. A number of kinetic studies have shown that the relative rates of ligand binding show ratios near 1.0 for a wide range of ligands.[1] At some point, however, steric factors at the metal site must become important and result in preferred "recognition" of selected substrates.

As part of a study of solution thermochemistry of organometallic complexes, we recently reported calorimetric and preliminary kinetic data[2] for the sterically crowded Kubas complex[3] shown in reaction 1. The emphasis of this earlier paper was on calor-

$$(P(C_6H_{11})_3)_2W(CO)_3(py) + P(OMe)_3 \rightarrow (P(C_6H_{11})_3)_2W(CO)_3(P(OMe)_3) + py \quad (1)$$

imetric determination of heats of ligand binding to $(P(C_6H_{11})_3)_2W(CO)_3$. The steric strain present in this formally "coordinatively unsaturated" complex is apparent in its structure and chemistry.[3] The sixth site of $(P(C_6H_{11})_3)_2W(CO)_3$ is occupied by a three-center W···H–C "agostic" bond. It thus represents a stable (but highly air-sensitive) complex analogous to proposed "agostic" intermediates in recent flash-photolysis studies such as those shown in eq 2 and 3.[4,5] Recent work has shown that the

$$Cr(CO)_6 \xrightarrow{h\nu} Cr(CO)_5 \xrightarrow{+C_6H_{12}} Cr(CO)_5(C_6H_{12}) \xrightarrow{+L} Cr(CO)_5(L) \quad (2)$$

$$DiphosMo(CO)_4 \xrightarrow{h\nu} DiphosMo(CO)_3 \xrightarrow{+toluene} DiphosMo(CO)_3(Tol) \xrightarrow{+L} DiphosMo(CO)_3(L) \quad (3)$$

"coordinatively unsaturated" complexes initially generated are rapidly solvated by alkane or arene solvents. It is normally the reactions of these complexes that are observed even on very fast time scales.[6] In this paper, we report new stopped-flow kinetic results that give a clear picture of ligand-substitution reactions in a sterically crowded environment. The complex $(P(C_6H_{11})_3)_2W(CO)_3$ displays, to our knowledge, the largest range of kinetic selectivity reported to date for such an organometallic complex.

Experimental Section

Manipulations involving organometallic complexes were performed under an argon atmosphere either by using standard Schlenk tube techniques or in a Vacuum/Atmospheres glovebox. Solvents were purified by distillation from an appropriate drying agent under an argon atmosphere. The complexes $(P(C_6H_{11})_3)_2W(CO)_3$ and $(P(C_6H_{11})_3)_2W(CO)_3(py)$ were prepared by literature methods.[3] The deuterium-substituted complex $(P(C_6D_{11})_3)_2W(CO)_3(D_2)$ was provided by Gregory J. Kubas, Los Alamos National Laboratory, and had isotopic purity greater than 98%. The complex $(P(C_6D_{11})_3)_2W(CO)_3$ was prepared from a solution of $(P(C_6D_{11})_3)_2W(CO)_3(D_2)$ in toluene that was evacuated to dryness, resulting in complete loss of coordinated D_2. The complex $(P(C_6D_{11})_3)_2W(CO)_3(py)$ was prepared from $(P(C_6D_{11})_3)_2W(CO)_3(D_2)$ by addition of pyridine. Kinetic measurements in this system required considerable effort. Slight impurities in either solvent or inert atmosphere lead to rapid decomposition of the very air-sensitive complexes. Kinetic measurements were made on a Hi-Tech SF-51 stopped-flow apparatus equipped with an SU-40 spectrophotometer unit. Infrared spectra were recorded on a Perkin-Elmer 1850 FTIR spectrophotometer. A typical procedure is described below and is representative of other measurements. Experimental errors on kinetic data are less than ±10% unless stated otherwise.

Measurement of the Rate of Reaction of $(P(C_6H_{11})_3)_2W(CO)_3$ and $(P(C_6D_{11})_3)_2W(CO)_3$ with $P(OMe)_3$. A solution that was approximately 5×10^{-4} M in the complex $(P(C_6H_{11})_3)_2W(CO)_3$ was prepared in the glovebox by dissolving 0.02 g of the complex in 50 mL of freshly distilled toluene. A second dilution was prepared from 0.100 mL of $P(OMe)_3$ in 25 mL of toluene, 3.4×10^{-2} M in phosphite. Both solutions were taken out of the glovebox, and the syringes in the stopped-flow apparatus were loaded by using a special manifold system designed to minimize exposure to the atmosphere. The syringes were flushed several times with the solution and then allowed to equilibrate at the bath temperature of 25 °C. After equilibration and firing two or three "shots" without recording the spectrum, data were accumulated for the run. The value for $t_{1/2}$ was 0.00075 s, corresponding to $k_{obsd} = 926$ for the pseudo-first-order rate constant $k_2[P(OMe)_3]$. Taking into account that the concentration of the stock solution is cut in half in the mixing process leads to calculation of the second-order rate constant of 5.46×10^4 M^{-1} s^{-1}. Reactions performed with different absolute values of phosphite concentration gave different pseudo-first-order rate constants, but values for the second-order rate constant agreed within experimental error. The syringes and stopped-flow apparatus were cleaned and loaded with the deuterium complex prepared under identical conditions. In order to insure that differences in rate for the isotopic studies were not due to small changes in the temperature of the bath or other sources of error, the measurements were made in an alternating sequence, hydrogen, deuterium, hydrogen, deuterium, etc. Results listed are the average of typically eight separate measurements.

Reactions of $(P(C_6H_{11})_3)_2W(CO)_3$ and PPh_3. A Schlenk tube was taken into the glovebox and loaded with 0.15 g of $(P(C_6H_{11})_3)_2W(CO)_3$ and 0.2 g of PPh_3. Addition of 10 mL of freshly distilled toluene resulted

(1) Darensbourg, D. J. *Adv. Organomet. Chem.* **1982**, *21*, 113 and references therein.
(2) Gonzalez, A. A.; Zhang, K.; Nolan, S. P.; de la Vega, R. L.; Mukerjee, S. L.; Hoff, C. D.; Kubas, G. J. *Organometallics* **1988**, *7*, 2429.
(3) Kubas, G. J. *Acc. Chem. Res.* **1988**, *21*, 120 and references therein.
(4) (a) Wang, L.; Xinming, Z.; Spears, K. G. *J. Phys. Chem.* **1989**, *93*, 2. (b) Wang, L.; Xinming, Z.; Spears, K. G. *J. Am. Chem. Soc.* **1988**, *110*, 8695.
(5) Asali, K. J.; van Zyl, G. J.; Dobson, G. R. *Inorg. Chem.* **1988**, *27*, 3313.
(6) For recent reviews in this area see: (a) Poliakoff, M.; Weitz, E. *Adv. Organomet. Chem.* **1986**, *25*, 277. (b) Weitz, E. *J. Phys. Chem.* **1987**, *91*, 3945.

0020-1669/89/1328-4285$01.50/0

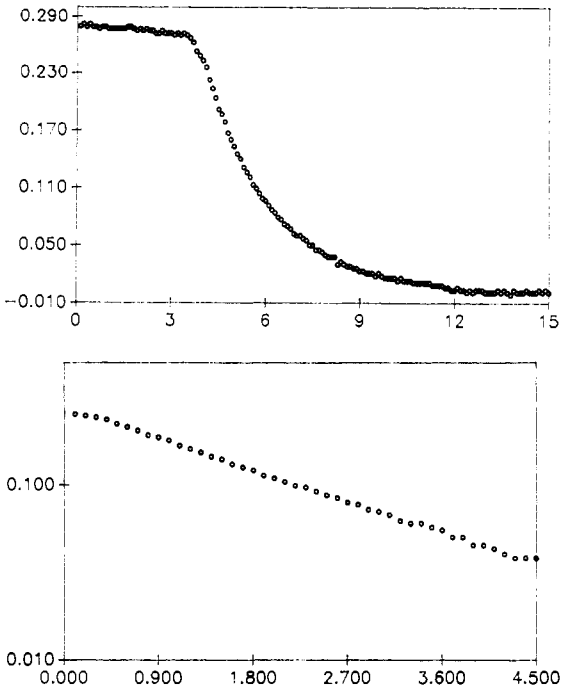

Figure 1. Plots of absorbance versus time (ms) on (a, top) linear and (b, bottom) logarithmic scales for the reaction of $(P(C_6H_{11})_3)_2W(CO)_3$ and $P(OMe)_3$ at 25 °C in toluene.

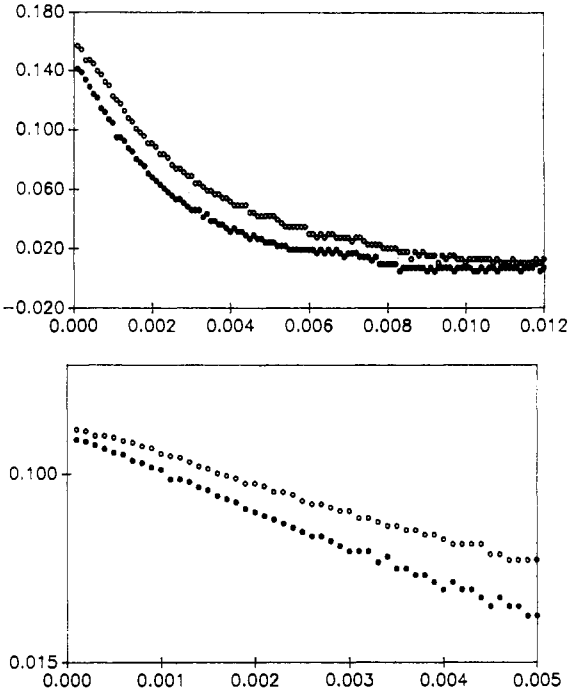

Figure 2. Plots of absorbance versus time (s) on (a, top) linear and (b, bottom) logarithmic time scales for the reactions of $(P(C_6H_{11})_3)_2W(CO)_3$ (○) and $(P(C_6D_{11})_3)_2W(CO)_3$ (●) with PPh_2Me at 25 °C in toluene.

in formation of an initially blue solution, which turned light yellow and then deposited a copious amount of light yellow precipitate within a few minutes. The solution was filtered and evaporated to dryness and the resulting solid then redissolved in C_6D_6. The presence of free PCy_3 was confirmed by ^{31}P NMR. The light yellow solid showed infrared bands (Nujol mull) at 1949 and 1846 cm^{-1} in agreement with an authentic sample of $(PPh_3)_3W(CO)_3$ prepared by reaction of $(CHPT)W(CO)_3$ (CHPT = cycloheptatriene) and excess PPh_3. Additional sealed-tube ^{31}P NMR experiments confirmed that 3 mol of PPh_3 react with 1 mol of $(PCy_3)_2W(CO)_3$ to generate the same solid precipitate and 2 mol of free PCy_3.

Results

Kinetic Measurements of Reaction of $(P(C_6H_{11})_3)_2W(CO)_3$ and $(P(C_6H_{11})_3)_2W(CO)_3$ with $P(OMe)_3$, PPh_2Me, 2,5-Me_2py, and py. Direct measurements of the second-order reactions of $(P(C_6H_{11})_3)_2W(CO)_3$ with ligands were made under pseudo-first-order conditions with at least a 20-fold excess of ligand. A typical experimental plot for reaction 4 is shown in Figure 1. Plots of

$$(P(C_6H_{11})_3)_2W(CO)_3 + P(OMe)_3 \rightarrow (P(C_6H_{11})_3)_2W(CO)_3(P(OMe)_3) \quad (4)$$

ln A were linear over 3–5 half-lives, as shown in Figure 1. An inverse kinetic isotope effect $k(H)/k(D) = 0.86$ was observed for reaction 4. A larger inverse kinetic isotope effect (0.77) was observed in the reaction with PPh_2Me:

$$(P(C_6H_{11})_3)_2W(CO)_3 + PPh_2Me \rightarrow (P(C_6H_{11})_3)_2W(CO)_3(PPh_2Me) \quad (5)$$

Typical linear and logarithmic plots for reaction 5 are shown in Figure 2 for the hydrogen- and deuterium-substituted complexes. The faster rate of reaction of the deuterium-substituted complex is apparent on visual inspection of the primary kinetic data. Second-order rate constants for reactions of $(P(C_6H_{11})_3)_2W(CO)_3$ with all ligands studied are collected in Table I. The reaction with 2,6-Me_2py was much slower and could be readily measured on the stopped-flow instrument.

$$(P(C_6H_{11})_3)_2W(CO)_3 + Me_2py \rightarrow (P(C_6H_{11})_3)_2W(CO)_3(Me_2py) \quad (6)$$

The steric influence of the two methyl groups was seen dramatically since reaction with pyridine, as shown in eq 7, was too

$$(P(C_6H_{11})_3)_2W(CO)_3 + py \rightarrow (P(C_6H_{11})_3)_2W(CO)_3(py) \quad (7)$$

rapid to follow accurately under pseudo-first-order conditions. The rate constant could be determined under second-order conditions. The ratio of the rate constants for reactions 4–7 can be determined by competition studies and are in agreement with the direct measurements.[7] Variable-temperature data for reaction 4, collected in Table I, allow calculation of the enthalpy of activation for this reaction of 4.2 ± 1.9 kcal/mol.

Table I. Rates of Reaction of $(P(C_6H_{11})_3)_2W(CO)_3$ and $(P(C_6D_{11})_3)_2W(CO)_3$ with Ligands[a]

ligand	T, °C	complex	k, M^{-1} s^{-1}
pyridine	25	H	1.0×10^{6} [b]
			8.7×10^{5} [c]
$P(OMe)_3$	35	H	6.5×10^{4}
$P(OMe)_3$	25	H	5.45×10^{4}
$P(OMe)_3$	25	D	6.25×10^{4}
$P(OMe)_3$	15	H	4.0×10^{4}
PPh_2Me	25	H	1.7×10^{4}
PPh_2Me	25	D	2.2×10^{4}
2,5-Me_2py	25	H	8.6×10^{3}

[a] Rates of reaction were measured under pseudo-first-order conditions as described in the Experimental Section. [b] The rate constant for this reaction was measured under second-order conditions. [c] Preferred value for rate of reaction, calculated from the rate of reaction with $P(OMe)_3$ and a k_{-1}/k_2 ratio of 16.

Data in Table I can be combined with data for reaction of H_2[7] to calculate the relative rates of reaction for $(P(C_6H_{11})_3)_2W(CO)_3$ which span over 2 orders of magnitude. The relative rates of reaction are in the order H_2 > py > $P(OMe)_3$ > PPh_2Me > 2,6Me_2py. These data are shown schematically in Figure 3.

Reaction of $(P(C_6H_{11})_3)_2W(CO)_3$ and PPh_3. As part of our attempts to map out the steric selectivity of $(P(C_6H_{11})_3)_2W(CO)_3$, we tried to investigate the kinetics of reaction 8 since PPh_3 had

$$(P(C_6H_{11})_3)_2W(CO)_3 + PPh_3 \rightarrow (P(C_6H_{11})_3)_2W(CO)_3(PPh_3) \quad (8)$$

been reported[3] to form a stable adduct. Unlike other reactions of $(P(C_6H_{11})_3)_2W(CO)_3$, which occur instantly upon mixing, reaction with PPh_3 occurred over a time scale of a few minutes.

(7) (a) Zhang, K.; Gonzalez, A. A.; Hoff, C. D. *J. Am. Chem. Soc.* **1989**, *111*, 3627. (b) Zhang, K.; Gonzalez, A. A.; Mukerjee, S. L.; Hoff, C. D. Unpublished results.

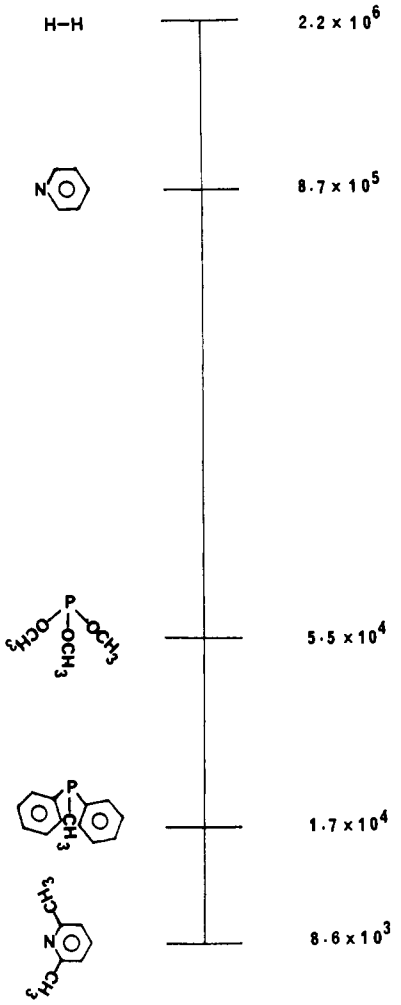

Figure 3. Relative rates of reactivity of selected ligands with $(P(C_6H_{11})_3)_2W(CO)_3$. The second-order rate constants (M^{-1} s^{-1}) for reaction at 25 °C are included beside each ligand on a logarithmic scale.

This reaction does not lead to the reported product shown in eq 8. Instead the reaction occurs as shown in eq 9.

$$(PCy_3)_2W(CO)_3 + 3PPh_3 \rightarrow (PPh_3)_3W(CO)_3 + 2PCy_3 \quad (9)$$

Kinetic Isotope Effects in Breaking the W–py Bond in $(P(C_6H_{11})_3)_2W(CO)_3(py)$ and $(P(C_6D_{11})_3)_2W(CO)_3(py)$. Earlier kinetic data[2] on reaction 1 lead to the mechanism shown in eq 10. The overall reaction was observed to be *slower* for the

$$(P(C_6H_{11})_3)_2W(CO)_3(py) \underset{k_{-1}}{\overset{k_1}{\rightleftharpoons}} py + (P(C_6H_{11})_3)_2W(CO)_3 + P(OMe)_3 \xrightarrow{k_2} (P(C_6H_{11})_3)_2W(CO)_3(P(OMe)_3) \quad (10)$$

deuterium-substituted complex; however, earlier data[2] did not allow evaluation of the individual rate constants in k_{obsd}. Application of the steady-state approximation for $W_k = (P(C_6H_{11})_3)_2W(CO)_3$ to the mechanism in eq 10 yields the rate law in eq 11. A plot

$$d[W_k\text{–}py]/dt = \frac{k_1k_2[W_k\text{–}py][P(OMe)_3]}{k_{-1}[py] + k_2[P(OMe)_3]} \quad (11)$$

of $1/k_{obsd}$ versus $[py]/[P(OMe)_3]$ should yield a straight line with slope k_{-1}/k_1k_2 and intercept $1/k_1$. Division of the slope by the intercept yields k_{-1}/k_2, the "selectivity" of the intermediate with regard to the two competing ligands. In our earlier work, only the slope of the line could be evaluated accurately. In order to determine the kinetic isotope effects at the intercept, data at low $[py]/[P(OMe)_3]$ ratios are required.

Typical kinetic data for reaction 10 in the absence of added pyridine are shown in Figure 4. These data obeyed first-order kinetics over at least 5 half lives. It is clear from Figure 4 that for dissociation of pyridine a *normal* kinetic isotope effect is observed compared to the *inverse* kinetic isotope effects clearly displayed in Figures 2 and 3 for the associative reactions. These new data, near the intercept, were essential to determine accurately the kinetic isotope effect. The new kinetic data at low pyridine concentrations are collected in Table II, together with some of the data reported earlier.[2] All data were analyzed by a computer least-squares analysis, and this results in slight changes from some of the earlier rate constants[2] that were determined graphically; however, none of these changes are outside experimental error. A plot of $1/k_{obsd}$ versus $[py]/[P(OMe)_3]$ is shown in Figure 5. These data are linear over nearly 2 orders of magnitude in $1/k_{obsd}$. The stopped-flow data fit well with the other data. The wide range studied for this reaction, combining conventional and stopped-flow studies, gives confidence to the proposed mechanism.

The combined data in Table II can be used to calculate the separate rate constants shown in Table III. Enthalpies of activation from the variable-temperature studies are collected in Table IV. We have reported previously that the enthalpy of reaction 12 is +19 ± 1 kcal/mol. Using only the activation data

$$(P(C_6H_{11})_3)_2W(CO)_3(py) \rightarrow (P(C_6H_{11})_3)_2W(CO)_3 + py \quad (12)$$

Table II. Rates of Reaction of $(P(C_6H_{11})_3)_2W(CO)_3(py)$ and $(P(C_6D_{11})_3)_2W(CO)_3(py)$ with $P(OMe)_3$ at Various $[py]/[P(OMe)_3]$ Ratios

T, °C	$[py]/[P(OMe)_3]$	$k_{obsd}(H) \times 10^3$, s^{-1}	$k_{obsd}(D) \times 10^3$, s^{-1}
35	0.00	450	373[a]
	0.194	140	93[a]
	0.905	35	30[b]
	1.81	16.8	14.5[b]
25	0.00	125.6	105.8[a]
	0.0997	49.8	42.5[a]
	0.199	27.3	24.0[a]
	0.398	18.8	16.4[a]
	0.875	8.67	7.40[b]
	1.75	4.24	3.79[b]
	3.50	2.29	1.95[b]
	4.50	1.73	1.49[b]
15	0.00	32.0	26.4[a]
	0.052	16.4	13.0[a]
	0.228	7.30	6.13[b]
	0.455	3.88	3.36[b]
	0.913	2.00	1.69[b]
	1.83	1.01	0.87[b]

[a] This work. [b] Data taken from ref 2.

Table III. Calculated Rate Constants for

$$W_k\text{–}py \underset{k_{-1}}{\overset{k_1}{\rightleftharpoons}} py + W_k + P(OMe)_3 \xrightarrow{k_2} W_k(P(OMe)_3)$$

$$W_k = (P(C_6H_{11})_3)_2W(CO)_3(py)$$

T, °C	complex	$k_{obsd} \times 10^3$, s^{-1}	k_1, s^{-1}	k_{-1}/k_2	$k_2 \times 10^{-4}$, M^{-1} s^{-1}
35	H	30.7	0.451	14.7	6.5
	D	27.5	0.373	13.5	
25	H	7.97	0.126	15.8	5.45
	D	6.81	0.106	15.5	6.25
15	H	1.90	0.032	16.8	4.0
	D	1.63	0.026	16.2	
5	H	0.436	0.0076	17.4	
	D	0.352	0.0063	18.0	

[a] Data calculated by using a least-square fit from data in Table II and ref 2. Data at 5 °C recalculated by using a least-squares fit instead of graphical treatment of data.[2]

Table IV. Calculated Activation Parameters (kcal/mol) for

$$W_k\text{–}py \underset{k_{-1}}{\overset{k_1}{\rightleftharpoons}} py + W_k + P(OMe)_3 \xrightarrow{k_2} W_k(P(OMe)_3)$$

$$W_k = (P(C_6H_{11})_3)_2W(CO)_3(py)$$

complex	$\Delta H^{\ddagger}_{k_1k_2/k_{-1}}$	$\Delta H^{\ddagger}_{k_1}$	$\Delta H^{\ddagger}_{k_2/k_{-1}}$	$\Delta H^{\ddagger}_{k_2}$
H	24.2 ± 0.2	23.4 ± 0.4	1.2 ± 0.2	4.2 ± 1.9
D	24.7 ± 0.3	23.4 ± 1.0	1.6 ± 0.5	

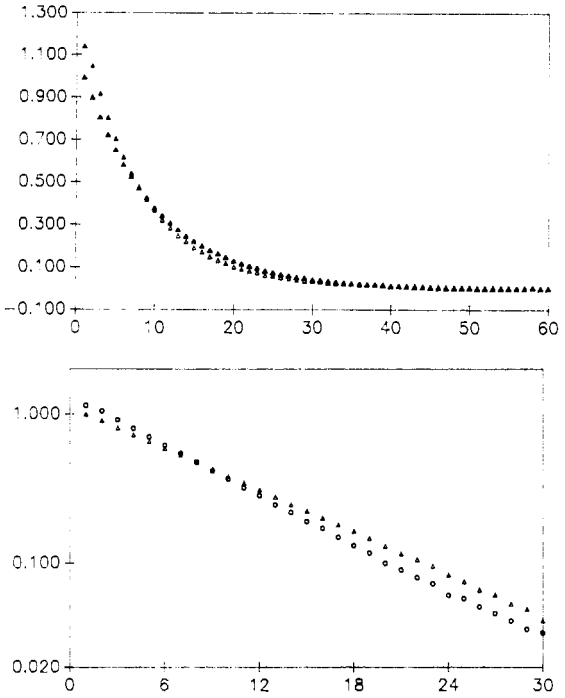

Figure 4. Plots of absorbance versus time (s) on (a, top) linear and (b, bottom) logarithmic time scales for reaction of $(P(C_6H_{11})_3)_2W(CO)_3(py)$ (○) and $(P(C_6D_{11})_3)_2W(CO)_3(py)$ (▲) (in the absence of added pyridine) with $P(OMe)_3$ at 25 °C in toluene.

in Table IV, the enthalpy of reaction 12 is calculated[8] to be +20.0 ± 2.1 kcal/mol. The two values, arrived at completely independently, agree within experimental error. The complete reaction profile for reaction 10 is shown in Figure 6.

Discussion

The initial goal of this work was to determine whether ligand dissociation in $(P(C_6H_{11})_3)_2W(CO)_3(py)$ was dissociative or intramolecular associative in nature. In view of the steric crowding around the metal, it seemed likely to us that our work would prove the reaction to be purely dissociative. This would allow comparison of the "thermodynamic" and "kinetic" bond strengths since only for purely dissociative reactions can such comparisons be made.[9] As discussed below, in spite of the steric crowding the reaction is at least partially associative in nature, complicating any such comparison.

Two limiting mechanisms can be imagined for reaction 12. The first involves pure dissociation in which the "agostic" bond is set up only after the pyridine ligand has effectively left the coordination sphere of tungsten as shown in eq 13. It would be expected,

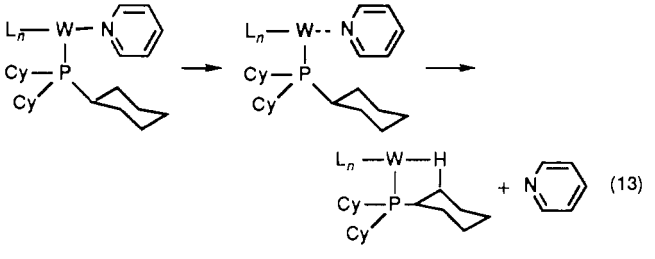

(13)

since the "agostic" bond is not involved in the transition state, that no kinetic isotope effect ($k(H)/k(D) = 1.0$) would be observed for this reaction. The second limiting case would involve an associative displacement in which the "agostic" bond is established at the transition state as shown in eq 14. The kinetic isotope effect

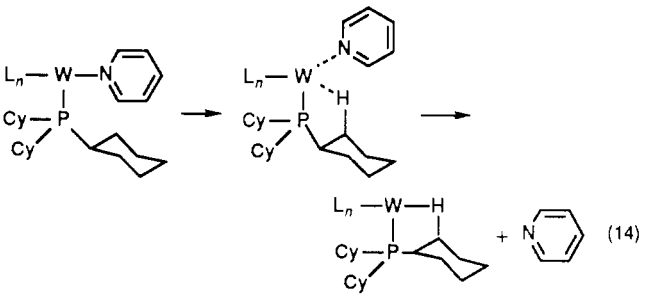

(14)

observed in this case would correspond to $K_{eq}(H)/K_{eq}(D)$, the equilibrium constant ratio for binding pyridine to the hydrogen-substituted and deuterium-substituted complexes. Kinetic isotope effects in alkane activation (which may involve agostic intermediates) have been recently discussed.[10,11]

As discussed in the Results, dissociation of pyridine shows a primary isotope effect, $k_1(H)/k_1(D) = 1.19$. The reverse reaction, ligand binding, shows an inverse kinetic isotope effect, $k_{-1}(H)/k_{-1}(D) = 0.87$. Since $k_1/k_{-1} = K_{eq}$, this implies that $K_{eq}(H)/K_{eq}(D) = 1.36$. Thus the hydrogen-substituted complex should be more extensively dissociated than the deuterium-substituted complex.

The favored dissociation from the hydrogen-substituted complex can be attributed to differences in the zero-point vibrational energy. A useful way to view this is in terms of the competition reaction shown in eq 15. In this reaction, it seems reasonable to assume

$$(P(C_6H_{11})_3)_2W(CO)_3(L) + (P(C_6D_{11})_3)_2W(CO)_3 \rightarrow (P(C_6H_{11})_3)_2W(CO)_3 + (P(C_6D_{11})_3)_2W(CO)_3(L) \quad (15)$$

that the W–L bond strengths should be the same. The difference in energy can be estimated on the basis of changes in the C–H and C–D vibrational frequencies during the reaction and is in rough agreement with the experimental value.[12] Preferred binding of ligands by the deuterium complex has been verified in separate experiments.[7b]

The kinetic isotope effect studies give insight into the detailed mechanism of the reaction. The fact that the kinetic isotope effect is roughly midway between the values expected for eq 13 and 14 gives strong support to a partially associative intramolecular ligand displacement. Thus, as shown in the potential energy diagram in Figure 6, the transition state is not directly above the starting materials since this would show a kinetic isotope effect in k_1 of 1.0. Neither is the transition state consistent with full establishment of the "agostic bond" since the kinetic isotope effect would then be 1.36. The observed value of 1.19 implies partial setup of the "agostic" bond in the transition state. Due to the principle

(8) The ground-state energy difference is the difference in activation energies between the k_1 and k_{-1} reactions. From the activation energy for k_2/k_{-1} being 1.2 ± 0.2 kcal/mol and the activation energy for k_2 being 4.2 ± 1.9 kcal/mol, it follows that the activation energy for k_{-1} is 3.0 ± 2.1 kcal/mol. Since the activation energy for k_1 is 23.4 ± 0.4 kcal/mol, the ground-state energy difference is calculated to be 20.4 ± 2.5 kcal/mol.

(9) In solution-phase work, "kinetic" bond strength estimates are generated from the temperature dependence of reaction rates and "thermodynamic" (or "calorimetric") bond strength estimates arise from measurements of the heat of mixing of two solutions.

(10) Buchanan, J. M.; Stryker, J. M.; Bergman, R. G. *J. Am. Chem. Soc.* **1986**, *108*, 1537.

(11) Parkin, G.; Bercaw, J. E. *Organometallics* **1989**, *8*, 1172.

(12) A rough estimate of the kinetic isotope can be made on the basis of the reduction in zero-point energy for the C–H and C–D bonds upon forming an "agostic" complex. Thus the normal C–H stretching frequency is around 2930 cm^{-1}, and it is reduced to about 2650 cm^{-1} in the "agostic" complex. The normal C–D stretch is around 2200 cm^{-1}, and assuming the "agostic" stretch is reduced proportionally, it should then appear at 2650 (2200/2930) cm^{-1} = 1990 cm^{-1}. Thus in reaction 14 as shown, the products would include a normal C–D stretch (2200 cm^{-1}) and an agostic C–H stretch (2650 cm^{-1}). The reactants would include a normal C–H (2930 cm^{-1}) and an agostic C–D stretch (1990 cm^{-1}). Thus there would be a net change in vibrational modes of −70 cm^{-1}. The zero-point energy change would then be half this value or −35 cm^{-1}, corresponding to about 0.1 kcal/mol as a driving force for the reaction. At room temperature, this would correspond to an equilibrium constant of about 1.2. This is a relatively crude analysis since not all the vibrational frequency changes are known; however, it is in rough agreement with the equilibrium data.

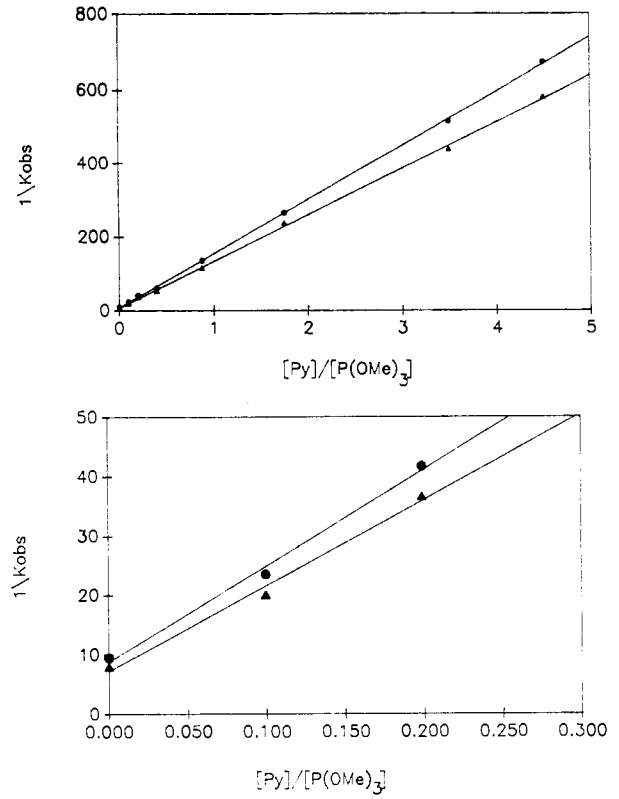

Figure 5. Plots of $1/k_{obsd}$ versus [py]/[$P(OMe)_3$] for the reaction: W_k–py + $P(OMe)_3$ → W_k–$P(OMe)_3$ + py (W_k = $(P(C_6H_{11})_3)_2W(CO)_3$) at 25 °C in toluene solution: (a) full-range plot; (b) expanded view near intercept.

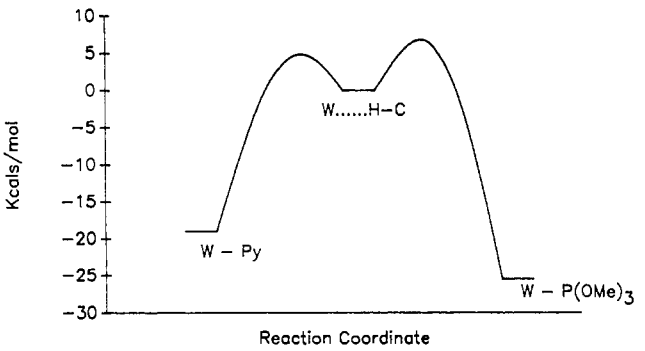

Figure 6. Potential energy diagram of the enthalpy of reaction for the reaction W_k–py → py + W_k + $P(OMe)_3$ → W_k–$P(OMe)_3$ (W_k = $(P(C_6H_{11})_3)_2W(CO)_3$).

of microscopic reversibility, attack of the incoming ligand on the "agostic" bond is also associative in nature. In view of the steric crowding around the metal center, this result was unexpected; however, there is precedent in the literature for this with less crowded metal centers.[13]

Relative rates of reaction of $(P(C_6H_{11})_3)_2W(CO)_3$ with various ligands are displayed in Figure 3. There is no apparent correlation between metal–ligand bond strengths and kinetics of the associative reaction. The order of bond strength data is H_2 < lutidine < py < PPh_2Me < $P(OMe)_3$.[2] The relative kinetic order, H_2 > py > $P(OMe)_3$ > PPh_2Me > 2,6-Me_2py, seems in keeping with intuitive feelings about the size of the incoming ligands.

The entire range of ligand selectivities in Figure 3 corresponds to only a 3.3 kcal/mol difference in the free energies of activation. *It seems most likely to us that the differences correspond to the placement of the transition state with regard to the extent to which the "agostic" bond is established.* For bulky ligands, the transition state is probably more fully dissociative in character. The smaller ligands may allow better establishment of the "agostic" bond, thus lowering the activation energy for ligand dissociation. Due to microscopic reversibility, the activation energy for ligand addition to $(P(C_6H_{11})_3)_2W(CO)_3$ would also be lower.

A different reaction course is followed by PPh_3. A possible mechanism for reaction 9 is shown in eq 16. While this reaction

$$(PCy_3)_2W(CO)_3 + PPh_3 \rightleftharpoons (PCy_3)_2W(CO)_3(PPh_3) \xrightarrow{-PCy_3} (PCy_3)W(CO)_3(PPh_3) \xrightarrow{+PPh_3} (PCy_3)W(CO)_3(PPh_3)_2 \xrightarrow{-PCy_3} W(CO)_3(PPh_3)_2 \xrightarrow{+PPh_3} W(CO)_3(PPh_3)_3 \quad (16)$$

is "slow" compared to the other reactions reported here, it is nevertheless complete within a few minutes of mixing the solutions. Spectroscopic attempts to detect intermediates were not successful.[7] It seems most likely that the reaction goes through a first step involving an unfavorable equilibrium to form the unstable complex $(PCy_3)_2W(CO)_3(PPh_3)$. Due to the severe steric crowding in this complex, dissociation of PCy_3 to form the mixed, coordinatively unsaturated complex $(PCy_3)W(CO)_3(PPh_3)$ is probably rapid. Addition of PPh_3 and replacement of the second PCy_3 yields the observed product. The relatively fast replacements of PCy_3 in this complex, out of keeping with normal substitution reactions for phosphine ligands,[1] attest to the importance of steric factors in this crowded complex. Dissociation of PCy_3 may be assisted by formation of an intramolecular agostic utilizing the arene C–H of PPh_3. It appears from the literature data that arenes form stronger M···H–C bonds than alkanes.[14] Regardless of the mechanism of the reaction, PCy_3 is ejected rapidly from the complex, and the reported complex[3] $(P(C_6H_{11})_3)_2W(CO)_3(PPh_3)$ is not formed in detectable amounts.

Conclusion

In spite of the steric crowding around the metal center, ligand-substitution processes in the complex W_k have been shown to be associative in nature. Kinetic isotope effect studies and arguments regarding the energy of reaction 2 indicate that the transition state involves substantial formation of the W···H–C bond prior to full dissociation of pyridine. The relatively rapid loss of what is normally a strong bond, W–py, may be the result of a smooth displacement by the agostic bond. In this view, the cyclohexyl group could be imagined to rotate into position and "knock on the door", encouraging the W–py bond to break.

Compared to related "agostic" complexes such as $Cr(CO)_5(C_6H_{12})$ the reactions of $(P(C_6H_{11})_3)_2W(CO)_3$ appear to be somewhat slower[13] and show higher ligand selectivity. No simple "bond strength" estimate can be made for $(P(C_6H_{11})_3)_2W(CO)_3(L)$ complexes. The reaction profile shown in Figure 6 gives our best view of ligand dissociation. Taken at face value, according to accepted definitions of bond strength estimates, a value of 19 kcal/mol should be given for the tungsten–pyridine bond strength, as depicted in eq 10. However, as discussed above, this is actually the difference in energy between the tungsten–pyridine and tungsten–"agostic" bond strengths. Since ligand displacement reactions in this system are not dissociative, kinetic data alone cannot yield an "absolute" value for the tungsten–pyridine bond strength. The bulky ligands, which create the steric crowding around the tungsten center and which would seem to prevent conventional associative reactions, actually participate in the intramolecular associative ligand interchange. This phenomenon may occur in other ligands containing bulky hydrocarbon ligands. The Kubas type complexes present a good opportunity for detailed study of these effects, and additional thermodynamic and kinetic studies are in progress on this and related complexes.

Acknowledgment. Support of this work by the National Science Foundation (Grant No. CHE-8618753) is gratefully acknowl-

(13) For example, the second-order rate constant for reaction of $Cr(CO)_5$(alkane) with CO is 3.6×10^6 M^{-1} s^{-1}: Church, S. P.; Grevels, F. W.; Hermann, H.; Schaffner, K. *Inorg. Chem.* **1985**, *24*, 418. This can be compared with our value for the reaction of $(P(C_6H_{11})_3)_2W(CO)_3$ with pyridine of 8.6×10^5 M^{-1} s^{-1}. Thus reaction of the tungsten complex is about 4 times slower than reaction of the chromium complex.

(14) Crabtree, R. H. *Adv. Organomet. Chem.* **1988**, *28*, 299.

edged. Special thanks are due to Dr. Gregory J. Kubas, Los Alamos National Laboratory, for a gift of $(P(C_6D_{11})_3)_2W(CO)_3(D_2)$ and also for helpful discussions. In addition, we wish to thank Dr. Nita A. Lewis and Daniel Taveras for allowing us to use the stopped-flow equipment.

Registry No. py, 110-86-1; 2,5-Me_2py, 589-93-5; $(P(C_6H_{11})_3)_2W(CO)_3$, 73690-56-9; $P(OMe)_3$, 121-45-9; PPh_2Me, 1486-28-8; $(P(C_6H_{11})_3)_2W(CO)_3(py)$, 100995-31-1; D_2, 7782-39-0.

Contribution from the Research Laboratories, Eastman Chemicals Division, Eastman Kodak Company, Kingsport, Tennessee 37662

Synthesis and Reactivity of Alkoxide-Bridged Cobaltic Acetates

Charles E. Sumner, Jr.,* and Guy R. Steinmetz

Received February 14, 1989

Several μ-alkoxy oxo-centered cobalt cluster complexes of formula $[(py)_3Co_3O(OAc)_5OR][PF_6]$, where R = methyl, ethyl, propyl, allyl, benzyl, and 3-phenylpropyl and py = pyridine, were synthesized by treatment of $[(py)_3Co_3O(OAc)_6][PF_6]$ with the alcohol. The 3-phenylpropyl complex [**7**] was characterized by X-ray crystallographic techniques. At 20 ± 1 °C, the crystal is monoclinic, with a = 35.684 (8) Å, b = 9.691 (3) Å, c = 27.134 (8) Å, β = 102.74 (2)°, V = 9152 (5) Å^3, Z = 8 [μ_a(Mo Kα) = 1.19 mm^{-1}; d_{calc} = 1.459 g cm^{-3}], and space group $C2/c$ (C_{2h}^6). The α-hydrogen atoms of the alkoxy ligand display chemical shifts of about 3 ppm upfield from that observed in the uncomplexed alcohol. The complexes decompose thermally to produce mixtures of the aldehyde and the acetate corresponding to the alkoxy ligand.

Introduction

Oxygen-bridged transition-metal cluster complexes are of interest for both theoretical and practical reasons.[1] These complexes offer a fundamental basis to study redox and ligand substitution reactions important to metal-catalyzed autoxidations. We have previously reported[2] the synthesis and dynamic behavior of several trinuclear oxo-centered and related hydroxy-bridged cobalt cluster complexes. The complexes represent the first trinuclear, oxo-centered cobalt clusters to be completely characterized. These complexes have been found to be interconvertable with one another depending upon the solvent medium.[3] Two of these complexes, $[(py)_3Co_3O(OAc)_6][PF_6]$ (**1**) and $[(py)_3Co_3O(OAc)_5OH][PF_6]$ (**2**) (py = pyridine), have been isolated from a cobalt-catalyzed autoxidation of alkylaromatics and are, themselves, catalytically active. The catalytic activity and dynamic behavior of these complexes suggest that they are actual catalyst intermediates and are thus excellent model complexes for the oxidation of organic substrates. Herein, we report the synthesis, characterization, and reactivity of a family of oxo-centered cobalt(III) cluster complexes bridged by alkoxide ligands as model compounds to study the oxidation of alcohols.

Experimental Section

Preparation of $[(py)_3Co_3O(OAc)_6][PF_6]$ (1). To a 250-mL flask were added $[(py)_3Co_3O(OAc)_5OH][PF_6]$ (**2**) (25.0 g, 0.028 mol), acetic acid (90 mL), and acetic anhydride (10 mL). The mixture was boiled for 5 min and allowed to cool to room temperature. The product was collected by filtration, washed with acetic acid (20 mL), and air-dried. The yield was 25.0 g (95%). Anal. Calcd for $C_{27}H_{33}Co_3F_6N_3O_{13}P$: C, 34.88; H, 3.55; N, 4.52. Found: C, 34.46; H, 3.40; N, 4.31. FAB/MS (positive mode) showed the molecular ion at m/e 784.

Preparation of $[(py)_3Co_3O(OAc)_5OCH_3][PF_6]$ (3). Method I. To a 125-mL Erlenmeyer flask equipped with a spin bar were added $[(py)_3Co_3O(OAc)_6][PF_6]$ (5.0 g, 5.4 mmol), acetonitrile (40 mL), and methanol (10 mL). The resulting mixture was boiled for 5 min and allowed to cool to room temperature. The solution was layered with diethyl ether (50 mL), and the flask was stoppered and allowed to stand overnight. The product was collected by filtration and air-dried. The yield was 3.9 g (80%). Anal. Calcd for $C_{26}H_{33}Co_3F_6N_3O_{12}P$: C, 34.63; H, 3.66; N, 4.66. Found: C, 34.33; H, 3.41; N, 4.50. FAB/MS showed the molecular ion at m/e 756. ^{13}C NMR (CD_2Cl_2): δ 49.6 (q, OCH_3, J_{CH} = 143 Hz).

Method II. To a 250-mL Erlenmeyer flask equipped with a spin bar was added $Co(OAc)_2{\cdot}4H_2O$ (10.0 g, 40.1 mmol) and 95/5 acetic acid/water (150 mL). Peracetic acid (4.0 mL; 40% solution) was added dropwise to the resulting mixture with stirring. An immediate color change from red to an olive green was observed. The solution was filtered with an additional 1.0 mL of peracetic acid added dropwise to the filtrate. The solution was stripped at room temperature under vacuum to give a green solid (6.91 g), which is crude "cobaltic acetate".

In a 250-mL Erlenmeyer flask equipped with a stir bar, "cobaltic acetate" (2.50 g) prepared from the above method was stirred in methanol (50.0 mL) for 5 min. Pyridine (0.98 g) was added to the reaction, which resulted in a rapid color change from green to brownish green. Addition of NH_4PF_6 (1.00 g), followed by a gentle refluxing for a few minutes, resulted in an immediate precipitation of a brown solid, which was isolated by filtration. Recrystallization of the brown solid in methylene chloride/pentane resulted in 0.34 g of $[(py)_3Co_3O(OAc)_5OCH_3][PF_6]$ with a trace (<1%) of $[(py)_3Co_3O(OAc)_5OH][PF_6]$ as judged by FAB/MS. ^1H and ^{13}C NMR spectra were identical with those of the product prepared from $[(py)_3Co_3O(OAc)_6][PF_6]$ and methanol.

Preparation of $[(py)_3Co_3O(OAc)_5OCH_2CH_3][PF_6]$ (4). To a 100-mL flask equipped with a reflux condenser and spin bar were added $[(py)_3Co_3O(OAc)_6][PF_6]$ (2.0 g, 2.2 mmol), acetonitrile (40 mL), and ethanol (10 mL). The mixture was heated at reflux for 10 min and allowed to cool to room temperature. The product crystallized as long, tan needles, and it was collected by filtration and vacuum-dried. The yield was 1.4 g (61%). Anal. Calcd for $C_{27}H_{35}Co_3F_6N_3O_{12}P$: C, 35.41; H, 3.83; N, 4.59. Found: C, 35.23; H, 3.81; N, 4.39. FAB/MS showed the molecular ion at m/e 770. $^{13}C\{^1H\}$ NMR (CD_3CN): δ 59.1 and 16.1 (s, 1 C each, OCH_2CH_3).

Preparation of $[(py)_3Co_3O(OAc)_5OCH_2CHCH_2][PF_6]$ (5). To a 100-mL flask equipped with a reflux condenser and spin bar were added $[(py)_3Co_3O(OAc)_6][PF_6]$ (2.1 g, 2.3 mmol), acetonitrile (40 mL), and allyl alcohol (10 mL). The resulting mixture was heated at reflux for 5 min and allowed to cool to room temperature. The solvent was evaporated, and the residue was taken up in methylene chloride, filtered, and layered with petroleum ether. After the mixture was left standing overnight, the product was collected by filtration. The yield was 1.5 g (72%). Anal. Calcd for $C_{28}H_{40}Co_3F_6N_3O_{12}P$: C, 36.05; H, 4.29; N, 4.51. Found: C, 35.29; H, 3.64; N, 4.47. FAB/MS showed the molecular ion at m/e 782. $^{13}C\{^1H\}$ NMR (CD_3CN): δ 136.2, 116.2, and 65.2 (s, 1 C each, OCH_2CHCH_2).

Preparation of $[(py)_3Co_3O(OAc)_5OCH_2C_6H_5][PF_6]$ (6). To a 100-mL flask equipped with a reflux condenser and spin bar were added

(1) (a) Meesuk, L.; Jayasooriya, U. A.; Cannon, R. D. *J. Am. Chem. Soc.* **1987**, *109*, 2009. (b) Sasaki, Y.; Tokiwa, A.; Ito, T. *J. Am. Chem. Soc.* **1987**, *109*, 6341. (c) Vincent, J. B.; Chang, H. R.; Folting, K.; Huffman, J. C.; Christou, G.; Hendrickson, D. N. *J. Am. Chem. Soc.* **1987**, *109*, 5703. (d) Oh, S. M.; Hendrickson, D. N.; Hasset, K. L.; Davis, R. E. *J. Am. Chem. Soc.* **1985**, *107*, 8009.

(2) (a) Sumner, C. E., Jr.; Steinmetz, G. R. *J. Am. Chem. Soc.* **1985**, *107*, 6124. (b) Sumner, C. E., Jr.; Steinmetz, G. R. *J. Catal.* **1986**, *100*, 549.

(3) Sumner, C. E., Jr., *Inorg. Chem.* **1988**, *27*, 1320 and references therein.

0020-1669/89/1328-4290$01.50/0